Effects of Reprocessing on Acrylonitrile–Butadiene–Styrene and Additives

Xiaojuan Bai (baixiaojuandh@163.com)
China University of Geosciences https://orcid.org/0000-0003-3274-6627
Pin Liang
Huazhong University of Science and Technology - Main Campus: Huazhong University of Science and Technology
Mei Zhang
Beijing Center for Physical and Chemical Analysis
Shiqiong Gong
Huazhong University of Science and Technology - Main Campus: Huazhong University of Science and Technology
Lihua Zhao
Huazhong University of Science and Technology - Main Campus: Huazhong University of Science and Technology

Research Article

Keywords: ABS, processing, 1H NMR, GPC, Py-GC/MS, degradation

Posted Date: June 2nd, 2021

DOI: https://doi.org/10.21203/rs.3.rs-539008/v1

Version of Record: A version of this preprint was published at Journal of Polymers and the Environment on October 21st, 2021. See the published version at https://doi.org/10.1007/s10924-021-02314-z.

Abstract

Acrylonitrile-butadiene-styrene (ABS) is one of the most extensively used engineering polymers and analysing the chemical structure changes during processing and recycling is extremely important. Hence, in this study, an ABS resin was processed using a torque rheometer at different temperatures and for different numbers of cycles. Pyrolysis gas chromatography mass spectrometry (Py-GC/MS) was used to study the effects of the processing parameters on additives. Fourier transform infrared spectroscopy (FTIR), hydrogen nuclear magnetic resonance (^{1}H NMR) spectroscopy, and gel permeation chromatography (GPC) were used to analyse the structural changes in the resin. GPC results showed that after processing at 290 °C using the torque rheometer, large size soluble polymeric components increased. The increase in the large size soluble polymeric components after processing at 290 °C was probably related to the crosslinking reactions in the grafted polybutadiene (PB). Furthermore, chemical analysis of the ABS resin samples after multiple extrusion cycles in a twin-screw extruder indicated that reprocessing considerably affected the ABS resin.

Introduction

Acrylonitrile-butadiene-styrene (ABS) is one of the most successful engineering thermoplastics. It comprises a dispersed phase containing polybutadiene (PB) rubber and a continuous rigid phase containing styrene-acrylonitrile (SAN) copolymer. The ABS resins used in this study were produced through the following process: Styrene and acrylonitrile monomers are grafted onto cross-linked PB latex particles to prepare a PB-g-SAN copolymer, and then the PB-g-SAN copolymer was blended with SAN to produce ABS. ABS resins usually contain lubricants and antioxidants.

ABS is also an interesting material to recycle. Extensive research has been conducted on ABS recycling. Casale et al. studied ABS degradation during processing as well as during ageing under natural and artificial light. They concluded that the toughness decreased mainly because of the degradation of the PB phase [1]. Eguiazábal and Nazábal studied the effects of repeated injection on the properties of polycarbonate (PC)/ABS blends at 260°C. They found that the rubber phase of ABS was cross-linked and oxidised [2]. Kim and Kang compared the effects of reprocessing on three types of ABS resins with different PB contents. They found that the impact strength of the ABS with the highest PB content was lowered more than those of the others [3]. Boldizar and Möller investigated the effects of combined extrusion and thermo-oxidative ageing on ABS and observed significant changes in the flow properties [4]. Bai et al. used a torque rheometer to reprocess ABS plastics at different temperatures and for different numbers of cycles. They attributed the reduction in impact strength to the degradation of the rubber phase [5]. Salari and Ranjbar studied the properties of ABS during reprocessing and thermo-oxidative ageing. They found that reprocessing and thermo-oxidative ageing had a much more severe effect on the impact strength than on the tensile strength [6]. Boronat et al. studied the effects of reprocessing on the processability of ABS. They found that the viscosity of low-viscosity ABS resins decreased and that of high-viscosity ABS resins increased [7]. Karahaliou and Tarantili studied the effects of reprocessing on ABS and ABS/montmorillonite nanocomposites [8, 9]. They found the elongation of ABS increased in the

third and forth cycles, and this result was similar to the result of Boldizar and Möller [4]. Pérez et al. found that the impact strength slightly decreased after reprocessing and that the number of reprocessing cycles had an obvious influence on the tensile strength during ultraviolet irradiation [10]. Peydro et al. reprocessed ABS at 220 and 260°C and then mixed the recycled ABS with styrene-ethylene/butylene-styrene copolymers. Their differential scanning calorimetry (DSC) results showed that the crosslinking reactions in the rubber phase caused a decrease in the crosslinking enthalpy, and this decrease was more apparent in the samples reprocessed at 260°C [11]. Scaffaro et al. studied the effect of the recycled ABS content and number of reprocessing cycles on the properties of ABS/recycled ABS blends [12]. Rahimi et al. blended virgin ABS with recycled ABS and studied the effect of reprocessing on the shrinkage and mechanical properties of the blend [13]. Hamarat et al. studied the influence of the number of recycling cycles on the properties of ABS. They prepared binary and ternary blends containing different weight percentages of virgin and recycled polymers. They found that the impact strengths of the blends with recycled ABS were lower than the impact strength of virgin ABS [14].

Many characterisation techniques are employed to examine the structures of polymers. Gas chromatography mass spectrometry (GC/MS) has previously been employed to study the effects of reprocessing on additives in ABS plastics [15]. Pyrolysis gas chromatography mass spectrometry (Py-GC/MS) has also been used in various aspects of polymer research including microstructure determination, degradation studies, and additive analysis [16]. Pentimalli et al. used hydrogen nuclear magnetic resonance (^{1}H NMR) spectroscopy to investigate the influence of γ irradiation on ABS [17].

ABS is one of the most important engineering polymers, and it is therefore important to carry out basic studies on the processing and recycling of ABS. Thus, in this study, we concentrated on analysing the effects of processing on the chemical structure of ABS. We used Py-GC/MS to study the effects of processing on additives. ^{1}H NMR was used to examine the changes in the chemical structure of ABS during processing. The Gel permeation chromatography (GPC) results obtained in our earlier work showed that the proportion of large size soluble polymeric components increased after processing at high temperature of 270°C, but the reason for that was not studied [5]. In another of our earlier works, we studied the mechanical properties of ABS during repeated extrusion [18], but we did not comprehensively analyse the chemical structure changes. To overcome these problems, the chemical changes in the structure of ABS during processing were further studied using several characterisation techniques in this work.

Material Processing

In this work, ABS is a commercially available material known as PA-757, produced by Chi Mei Corp. (Taiwan).

Melt processing of the polymers was conducted using a torque rheometer. The ABS raw material (sample code ABS0) was dried in an oven at 80°C for 2 h before processing. When the temperature in the cavity of the torque rheometer reached 230°C, 60 g of the ABS raw material was placed in the cavity, and a time of

3 min was allowed for the cavity temperature to stabilise. Then, the material was processed at 30 rpm for 10 min. After processing, the blades were stopped, the cavity was opened at 230°C, and approximately 10 g of material was removed (sample code ABS-L1). Subsequently, the cavity was closed, the remaining material was processed at 30 rpm for another 10 min at 230°C; the cavity was opened, and approximately 10 g of ABS was again removed from the cavity (sample code ABS-L2). The cavity was closed again, the remaining material was processed for another 10 min at 230°C, and all the processed material was then removed from the cavity (sample ABS-L3). Another batch of the ABS resin was processed at 290°C for one, two, and three cycles using the same method, and the corresponding samples were designated as ABS-H1, ABS-H2, and ABS-H3, respectively. One ABS sample was also processed at 260°C for one cycle (sample ABS-M1). Table 1 presents the number of processing cycles and processing temperatures for each sample processed using the torque rheometer.

Table 1
Number of processing cycles and processing temperatures for samples

Sample code	Number of processing cycles	Processing temperature (°C)
ABS0	0	
ABS-L1	1	230
ABS-L2	2	230
ABS-L3	3	230
ABS-M1	1	260
ABS-H1	1	290
ABS-H2	2	290
ABS-H3	3	290

Another set of samples was prepared from the ABS raw material, which was processed using a twin-screw extruder over a period of time. In March 2009, the ABS was reprocessed using a twin-screw extruder. The following extruder temperature profile was used for reprocessing ABS: 190, 205, 205, 205, 205, 205, and 205°C. After each extrusion cycle, the extrudate was cooled using water and pelletised. Some of the pellets were moulded into samples using an injection moulding machine at 190–210°C, and the other pellets were processed again in the next extrusion cycle. Sample ABS-E0 was prepared by moulding the ABS raw material in the injection moulding machine without subjecting it to extrusion. Before extrusion and injection moulding, the raw material was heated at 80°C for approximately 5 h in an air oven.

In March 2019, following preservation in the dark at room temperature for 10 years, some injection-moulded samples were aged in a thermal ageing test chamber at 110°C for 21 days. Before thermo-oxidative ageing, the surfaces of these samples were ground using sandpaper. Table 2 mentions the

number of extrusion cycles and ageing times for each representative sample prepared through extrusion and injection moulding.

Table 2
Number of extrusion cycles and ageing times for representative samples

Sample code	Number of extrusion cycles	Ageing time
ABS-E0	0	0
ABS-E1	1	0
ABS-E5	5	0
ABS-E0N	0	10-year preservation
ABS-E5N	5	10-year preservation
ABS-E0NA	0	10-year preservation and 21-day accelerated ageing
ABS-E5NA	5	10-year preservation and 21-day accelerated ageing

Characterization

Hydrogen nuclear magnetic resonance spectroscopy

ABS samples (0.6 g) were added to 10 mL of $CDCl_3$ containing tetramethylsilane (TMS) as the internal reference (Aldrich) and kept for one day to dissolve the materials; the mixtures were then filtered through a 0.2-μm syringe filter. The suspensions before and solutions after filtering were analysed at 25°C using an NMR system (AVANCE III HD 600M Hz, Bruker Company, Switzerland). Figure 1 shows photographs of the some samples. The suspensions of ABS are on the right, and their filtrates are on the left.

Fourier transform infrared spectroscopy

ABS samples (0.6 g) were added to 10 mL of $CDCl_3$ and kept for one day to dissolve the ABS. Then, the formed suspensions were filtered through a 0.2-μm syringe filter; the suspensions before and solutions after filtering were formed into films and examined using an FTIR system (VERTEX 70, Bruker, Germany).

The absorbance of *trans*-1,4-PB components at 967 cm^{-1} and that of 1,2-PB components at 1636 cm^{-1} were compared with the absorbance of PS components at 1602 cm^{-1}: Y_1 = Absorbance at 967 cm^{-1}/Absorbance at 1602 cm^{-1}; Y_2 = Absorbance at 1636 cm^{-1}/Absorbance at 1602 cm^{-1}.

Gel permeation chromatography

GPC analysis was conducted using an Agilent 110 instrument (Agilent, USA). The ABS samples (30 mg) were added to tetrahydrofuran (THF, 15 ml) to prepare sample solutions. The mixtures were kept for one

day to dissolve the ABS. The solutions thus obtained were filtered through a 0.2-μm syringe filter prior to conducting chromatography. The molecular weight distribution was determined at 30°C using a PLgel column (Mixed-C, 300 × 7.5 mm, 5-μm particle size) using a refractive index detector. THF was used as the eluent at a flow rate of 1.0 mL/min. The GPC system was calibrated with polystyrene (PS) standards.

Pyrolysis gas chromatography mass spectrometry

For each run, the sample was placed in a pyrolyser (EGA/PY-3030D, Frontier Lab, Japan) and heated at 300°C for 1 min. The volatiles were carried by He gas (0.8 mL/min) through a column (Ultra-5,30 m × 0.25 mm × 0.25 μm) of a gas chromatograph-mass spectrometer (QP2010-Ultra, Frontier Lab, Japan). The oven temperature was held at 40°C for 1 min, then increased at 8°C/min to 300°C, and held for 10 min. The split/splitless injector was used in the split mode with a split ratio of 5:1. Each component was analysed using an MS detector with an electron impact source and a mass range of m/z = 29–1000. The interface and source temperatures were 280 and 200°C, respectively. The NIST 05 Library of Mass Spectra was used for identifying the compounds.

Dynamic mechanical thermal analysis (DMTA)

A dynamic mechanical thermal analyser (DMA8000, PE Company, USA) was employed to test the samples using a single cantilever-type clamp configuration at a frequency of 1 Hz, with a heating rate of 5°C/min. The surfaces of the injection-moulded samples were ground before conducting DMTA measurements. The test samples were approximately 10.0-mm long, 7.7-mm wide, and 2.3-mm thick. They were much smaller than the original impact testing samples (10.0-mm wide and 4.0-mm thick), and were extracted from central parts of the original samples.

Melt flow rate (MFR) measurements

The MFR was measured by a melt flow indexer (SRZ- 400C, Changchun Intelligent Instrument & Equipment Company, China). The test temperature was 230°C. The load was 5.0 kg. The MFR is defined as

$$\mathrm{MFR} = \frac{W}{t} \times 600$$

where W is the extrudate weight in grams within a time t of 10 s. Therefore, the units of MFR are g (10 min)$^{-1}$.

Results And Discussion

Py-GC/MS analysis

Figure 2 shows the total ion chromatograms of virgin ABS (ABS0), ABS processed at 230 (ABS-L1), 260 (ABS-M1), and 290 °C (ABS-H1) obtained via Py-GC/MS. At retention times of 22–23 min, there is a

complex of several overlapping peaks, among which Peak 3, Peak 4, and Peak 5 are prominent. They all show a molecular ion at m/z = 210, corresponding to a trimer derived from two acrylonitrile units and one styrene unit. Another group of peaks with retention times of 25.2–25.7 min, including Peak 14, Peak 15, and Peak 16, show a molecular ion at m/z = 261, corresponding to a trimer derived from two styrene units and one acrylonitrile unit [19, 20]. The changes in these peaks after processing at different temperatures were relatively small, probably because all of the above mentioned peaks originated from the SAN phase, which was relatively stable during processing.

Some other compounds that were confirmed by referring to the NIST 05 Library of Mass Spectra are shown as numbered peaks in Figure 2. Peak 26 at 37.82 min, corresponds to antioxidant 1076 (octadecyl 3-(3,5-di-*tert*-butyl-4-hydroxyphenyl)propionate). Peak 6 at 23.33 min is related to 1-octadecanol, which formed during the decomposition (hydrolysis) of antioxidant 1076 [21]. Interestingly, the size of the 1-octadecanol peak originating from ABS-M1 was lower than that originating from any of the other samples analysed. Therefore, during processing at 260 °C, the rate of decomposition of 1076 was slower than the rate of volatilisation of 1-octadecanol. Octadecanenitrile (Peak 7 at 23.62 min) and hexadecanenitrile (Peak 2 at 21.20 min) could be the decomposition products of ethylene bis(stearamide) (EBS), used as a lubricant [15]. These peaks became much larger in the spectra obtained for the samples processed at a higher temperature, suggesting that EBS could decompose when processing at higher temperatures. The increases of Peaks 12, 17, 18, 19, and 21 indicates some other additives decomposed at 290 °C.

Figure 3 shows the total ion chromatograms of virgin ABS (ABS0), and ABS processed at 230 °C for different numbers of cycles using the torque rheometer. It can be seen that the 1-octadecanol (Peak 6 at 23.33 min) did not increased during reprocessing. The content of octadecanoic acid (Peak 13 at 24.52 min) was reduced after reprocessing. After processing at 230 °C for three cycles, the peak of antioxidant 1076 (Peak 26 at 37.82 min) was still a large peak.

Effects of reprocessing using the torque rheometer

The ABS samples after processing at 230 °C for one cycle (ABS-L1), 230 °C for three cycles (ABS-L3), and 290 °C for one cycle (ABS-H1) were dissolved in $CDCl_3$. After filtration through a membrane, the filtrates were all colourless and transparent (see Figure 1).

Figure 4(a) shows the FTIR spectra of ABS-L1 before (red line) and after filtration (blue line). The solvent used was $CDCl_3$ containing a small amount of TMS. The $CDCl_3$ with TMS were evaporated before the IR spectra were recorded, but the spectrum of residual solvent (green line) shows two peaks originating from $CDCl_3$ (at 745 and 913 cm^{-1}). However, these solvent peaks did not affect the study of ABS degradation in this work. Before filtration, the peaks corresponding to aromatic and aliphatic C-H stretching vibrations are at 3200–3000 cm^{-1} and 3000–2800 cm^{-1}, respectively. The stretching vibration of C≡N appears at 2240 cm^{-1}. The peak at 1636 cm^{-1} is attributed to the stretching vibration of the double bonds in the 1,2-PB components. The peaks attributed to the stretching vibrations of the double bonds in the aromatic

rings of the styrene-derived components are at 1602 and 1493 cm^{-1}. The peak at 1028 cm^{-1} is also attributed to the aromatic rings derived from styrene. The peak corresponding to the out-of-plane bending vibration of the hydrogen atoms in the C-H groups attached to the alkenic carbons in *trans*-1,4-PB components is observed at 967 cm^{-1}. The peaks at 762 and 702 cm^{-1} are related to the out-of-plane bending of the C-H groups in the aromatic rings [22, 23]. Comparing the spectrum of ABS-L1 after filtration with that before filtration, three peaks nearly disappeared after filtration, two of which were related to *trans*-1,4-PB components (967 cm^{-1}) and 1,2-PB components (1636 cm^{-1}). The third peak was at 3301 cm^{-1} and may be attributed to hydroxyl groups introduced during the oxidation or hydration of the rubber phase. The other peaks exhibited minimal changes after filtration. From Figure 4(a), the rubber particles were filtered out from the suspension as they were not soluble in $CDCl_3$.

Figure 4(b) presents the FTIR spectra of the ABS suspensions after processing for one cycle at 230 and 290 °C. There are only minor differences between the spectra of ABS-L1 and ABS-H1.

The ^1H NMR spectra of ABS-L1, ABS-L3, and ABS-H1 before filtration are shown in Figure 5(a). The peaks at 4.8–5.0 and 5.5 ppm correspond to the vinyl units (—$CH=CH_2$) of the 1,2-PB components, and the peak at approximately 5.4 ppm corresponds to the hydrogens in the 1,4-PB units (—CH=CH—) [24-26]. The peaks at 6.5–7.5 ppm correspond to the protons of the styrene-derived phenyl rings, and those at 1.0–3.0 ppm are attributed to the protons of the saturated units (CH_2 and CH groups). In particular, the peaks at 1.9–2.1 ppm are mainly related to the CH_2 protons in the 1,4-PB units [26, 27]. Figure 5(a) shows that all the peaks of the PB units have become smaller after processing at a higher temperature of 290 °C. Compared to processing at 230 °C for three cycles, processing at 290 °C for one cycle caused a greater reduction in the sizes of the signals at 1.9–2.1 and 4.8–5.5 ppm. This is consistent with the rubber phase of ABS undergoing crosslinking at high processing temperatures [5]. Crosslinking within the rubber phase can reduce the solubility of PB. Figure 5(a) also shows that the relative intensity of the sharp peak at 1.19 ppm increases after processing at 290 °C. This peak probably arises from antioxidants and/or lubricants [28], which are compounds with long-chain alkyl groups added to the resin during manufacture. Degradation of these additives could yield molecules that are more easily soluble in $CDCl_3$.

The ^1H NMR spectra of the filtrates of ABS-L1, ABS-L3, and ABS-H1 are shown in Figure 5(b). Here, the peaks at 5.34 and 5.31 ppm, corresponding to the protons in *trans*-1,4-PB and *cis*-1,4-PB, respectively, are much smaller than the peaks observed in this region prior to filtration, confirming the removal of most of the rubber phase during filtration. After filtration, the sizes of the peaks at 1.9–2.1 ppm also decreased, and two small peaks at 2.01 and 1.96 ppm simultaneously became more apparent. The peaks at 2.01 and 1.96 ppm originated from the —CH_2— protons in *cis*-1,4-PB and *trans*-1,4-PB components, respectively [26], considering that a small amount of PB was originally grafted onto SAN. When the ABS solution was filtered, the grafted PB molecules may have moved into the filtrate even though the PB rubber phase was removed. Figure 5(b) also reveals that the peaks at 2.01 and 1.96 ppm are reduced after processing at 230 °C for three cycles and at 290 °C for one cycle. One likely reason for this reduction

is thermo-oxidative degradation of the grafted PB. Another possibility is that the grafted material itself, i.e. PB, underwent crosslinking. The prominent sharp peak at approximately 1.5 ppm probably originated from a small quantity of water entering the filtrate during filtration.

ABS samples processed using the torque rheometer were dissolved in THF and were filtered through a 0.2-μm syringe filter. The rubber particles were filtered out as they were not soluble in THF [29]. The molecular weight distribution of soluble components of the filtrate was analysed using GPC. Some of the recorded GPC curves are shown in Figure 6. The first broad peak represents the higher-molecular-weight polymeric components, and the second peak represents lower-molecular-weight components. The weight-average molecular weights (M_w) of the polymeric (macromolecular) components were calculated considering the section between the two red vertical lines. As shown in Figure 6, reprocessing at 230 °C for three cycles using the torque rheometer has a minimal influence on the size distribution of the macromolecular portion. From Figure 5(a), it can be known that the crosslinking reactions did not extensively happen in rubber phase during reprocessing at 230 °C. In our earlier work [5], a recycled ABS plastic was reprocessed at 230 °C using a torque rheometer. Dynamic mechanical thermal analysis (DMTA) reflected the occurrence of crosslinking reactions in PB phase. At the same time, GPC results showed that the proportion of large size soluble polymeric components slightly increased. Based on these works, it is suggested that the increase in the proportion of large size soluble polymeric components during reprocessing in our earlier work was possibly caused by crosslinking reactions in the grafted PB.

The GPC curves for the soluble components of ABS0 and ABS-H3 are shown in Figure 7. It is evident that the large size soluble polymeric components increase after reprocessing at 290 °C for three cycles. Figure 8 presents the M_w of the soluble polymeric components determined for the ABS. It is apparent that the M_w increases substantially during the first and second processing cycles. In the subsequent processing cycles, the M_w increased to a lesser extent. When the number of double bonds remaining to participate in the crosslinking reactions during the subsequent cycles decreased [11], the increase in the M_w became slow.

Effects of repeated extrusion and thermo-oxidative ageing

Ten years ago, prior to the present study, Bai et al. processed virgin ABS through extrusion for five cycles using a twin-screw extruder at 205 °C, and the mechanical properties were measured after the various reprocessing cycles [18]. In the present research, the chemical changes in the structure of ABS during repeated extrusion were further studied.

As shown in Figure 9, reprocessing at 205 °C for five cycles using the twin-screw extruder had a small influence on the size distribution of the macromolecular portion. The GPC results obtained 10 years ago show that the proportion of large size polymeric components and small size polymeric components slightly increased. Based on analysis above, it can be suggested that crosslinking reactions occurred in

the grafted PB. Our results show a slight increase in MFR (melt flow rate) after repeated extrusion (Figure 10). One reason for the increase in MFR could be breaking of the grafts between PB and SAN [4].

In our early work, we studied the mechanical properties of ABS during repeated extrusion [18]. Some results are shown again in Figure 11. From Figure 11, impact strength decreased and elongation increased after reprocessing. Degradation of the grafts between PB and SAN could be an important reason for the decrease in impact strength. Crosslinking reactions in the grafted PB may explain the increase in elongation, because the relationships between SAN phase and PB phase became strong.

In the present research, to study the changes in the chemical structure of ABS during thermo-oxidative ageing, some injection-moulded samples were placed in a thermal ageing test chamber at 110 °C for 21 days. Accelerated thermo-oxidative ageing was performed 10 years after the samples were fabricated. During these 10 years, the samples were preserved at room temperature without light exposure. Although the samples had been stored in sealed plastics bags, the surfaces of the samples were ground with sandpaper before thermo-oxidative ageing to reduce the effects of natural ageing on the test results.

Figure 12 shows the variations in the storage modulus (E') and loss modulus (E'') *versus* temperature for ABS-E0N and ABS-E5N. The plots of E'' against temperature shows that the lower temperature transition due to the rubber phase is slightly shifted to higher temperatures after repeated extrusion, suggesting the occurrence of crosslinking reactions in the rubber phase. The higher temperature transition due to the SAN phase shows no significant change [30]. Furthermore, the DMTA results presented in Figure 13 prove that reprocessing has a considerable influence on the chemical structure of ABS. The apparent change after the multiple extrusion and thermo-oxidative ageing may reflect the loss of the antioxidant during the extrusion cycles.

The Py-GC/MS results for these samples were obtained using another Py-GC/MS system under conditions similar to those used for the other samples (Figure 14). From Figure 14, we can find some fatty compounds (e.g. hexadecanoic acid) were lost after reprocessing. Some fatty compounds were oxidised during thermo-oxidative ageing. For example, *N*-(2-hydroxyethyl) hexadecanamide was found formed during thermo-oxidative ageing.

Conclusions

We comprehensively studied the changes in the chemical structures of an ABS resin using NMR, FTIR, GPC, and Py-GC/MS.

The ^{1}H NMR spectra of ABS suspensions showed that during processing at 290 °C using a torque rheometer, changes in the structure of the PB phase occurred, the reduction in the intensities of the ^{1}H NMR peaks corresponding to PB was mainly attributed to the crosslinking reactions within the PB phase. The M_w increases substantially during the first and second processing cycles. In the subsequent processing cycles, the M_w increased to a lesser extent. According to all the results we obtained, we concluded that the increase in large size soluble polymeric components during processing was probably

caused by crosslinking reactions in the grafted PB. In this study, reprocessing at 230 °C using the torque rheometer had a slight influence on PB and SAN of ABS, but the thermo-oxidative degradation of the grafted PB possibly occurred. Some additives tended to decompose during processing at 290 °C.

In our study, elongation increased after reprocessing using a twin-screw extruder, the reason for that may the crosslinking reactions in the grafted PB. However, impact strength decreased after reprocessing, thermo-oxidative degradation of the grafted PB may be an important reason. After repeated extrusion, the rubber phase of ABS was more easily oxidised during thermo-oxidative ageing. The apparent change of PB units after the multiple extrusion and thermo-oxidative ageing may reflect the loss of the antioxidant during the extrusion cycles. During reprocessing, some fatty compounds (e.g. hexadecanoic acid) were lost, and some fatty compounds were oxidised during thermo-oxidative ageing.

Declarations

Acknowledgements

We thank the following people for their assistance: Keith Smith at Cardiff University and David H. Isaac at Swansea University in United Kingdom; Shan Hu and her students, Yifan Chen, et al. at China University of Geosciences; Wenyi Chen at Wuhan University of Technology; Shiqiong Gong, Lihua Zhao, and Hong Cheng at Huazhong University of Science and Technology; Yingjie Shi at Beijing Center for Physical and Chemical Analysis.

References

1. Casale A, Salvatore O, Pizzigoni G (1975) Measurement of aging effects of ABS polymers. *Polym Eng Sci* 15: 286-293.
2. Eguiazábal JI, Nazábal J (1990) Reprocessing polycarbonate/acrylonitrile-butadiene-styrene blends: Influence on physical properties. *Polym Eng Sci* 30: 527-531. https://doi.10.1002/pen.760300905.
3. Kim JK, Kang CK (1995) Basic studies on recycling of ABS resin. *Polym-PlastTechnol Eng* 34: 875-590. https://doi.10.1080/03602559508012182.
4. Boldizar A, Möller K (2003) Degradation of ABS during repeated processing and accelerated ageing. *Polym DegradStabil* 81: 359-366. https://doi. 10.1016/S0141-3910(03)00107-1.
5. Bai X, Isaac DH, Smith K (2007) Reprocessing acrylonitrile-butadiene-styrene plastics: Structure-property relationships. *Polym Eng Sci* 47: 120-130. https://doi. 10.1002/pen.20681.
6. Salari D, Ranjbar H (2008) Study on the recycling of ABS resins: Simulation of reprocessing and thermo-oxidation. *Iran Polym J* 17: 599-610.
7. Boronat T, Segui VJ, Peydro MA, Reig MJ (2009) Influence of temperature and shear rate on the rheology and processability of reprocessed ABS in injection molding process. *J Mater Process Tech.* 209: 2735-2745. https://doi. 10.1016/j.jmatprotec.2008.06.013.

8. Karahaliou E-K, Tarantili PA (2009) Stability of ABS compounds subjected to repeated cycles of extrusion processing. *Polym Eng Sci* 49: 2269-2275. https://doi.10.1002/pen.21480.
9. Karahaliou E-K, Tarantili PA (2009) Preparation of poly(acrylonitrile-butadiene-styrene)/montmorillonite nanocomposites and degradation studies during extrusion reprocessing. *J Appl Polym Sci* 113: 2271-2281. https://doi.10.1002/app.30158.
10. Pérez JM, Vilas JL, Laza JM, Arnáiz S, Mijangos F, Bilbao E, León LM (2010) Effect of reprocessing and accelerated weathering on ABS properties. *J PolymEnviron* 18: 71-78. https://doi. 10.1007/s10924-009-0154-7.
11. Peydro MA, Parres F, Crespo JE, Navarro R (2013) Recovery of recycled acrylonitrile-butadiene-styrene, through mixing with styrene-ethylene/butylene-styrene *J Mater Process Tech* 213: 1268-1283. https://doi. 10.1016/j.jmatprotec.2013.02.012.
12. Scaffaro R, Botta L, Di Benedetto G (2012) Physical properties of virgin-recycled ABS blends: Effect of post-consumer content and of reprocessing cycles. *Eur Polym J* 48: 637-648. https://doi. 10.1016/j.eurpolymj.2011.12.018.
13. Rahimi M, Esfahanian M, Moradi M (2014) Effect of reprocessing on shrinkage and mechanical properties of ABS and investigating the proper blend of virgin and recycled ABS in injection molding. *J Mater Process Tech* 214: 2359-2365. https://doi. 10.1016/j.jmatprotec.2014.04.028.
14. Hamarat I, Kuram E, Ozcelik B (2018) Investigation the mechanical, rheological, and morphological properties of acrylonitrile butadiene styrene blends with different recycling number content.*Proc IMechE Part E: J Process Mech Eng* 232: 449-458. https://doi. 10.1177/0954408917717994.
15. Bai X, Stein BK, Smith K, Isaac DH (2012) Effects of reprocessing on additives in ABS plastics, detected by gas chromatography/mass spectrometry. *Prog Rubber Plast Re* 28: 1-14.
16. Yang R, Zhao J, Liu Y (2013) Oxidative degradation products analysis of polymer materials by pyrolysis gas chromatography-mass spectrometry. *Polym Degrad Stabil* 98: 2466-2472. https://doi. 10.1016/j.polymdegradstab.2013.05.018.
17. Pentimalli M, Capitani D, Ferrando A, Ferri D, Ragni P, Segre AL (2000) Gamma irradiation of food packaging materials: An NMR study. *Polymer* 41: 2871-2881. https://doi. 10.1016/S0032-3861(99)00473-5.
18. Bai X, Wu Z, and Feng N (2012) Degradation of ABS in ABS/$CaCO_3$ composites during reprocessing. *Adv Mater Res* 455-456: 845-850. https://doi.10.4028/scientific5/AMR.455-456.845
19. Shapi MM, Riekkola M-L (1992) Chemical ionization mass spectrometry and gas chromatographic identification of some nitrogen-containing volatile compounds from large-scale pyrolysis of poly (acrylonitrile-butadiene-styrene) plastics. *J Microcol Sep* 4: 35-43. https://doi.10.1002/mcs.1220040108.
20. Bozi J, Czégény Z, Blazsó M (2008) Conversion of the volatile thermal decomposition products of polyamide-6, 6 and ABS over Y zeolites. *Thermochim Acta* 472: 84-94. https://doi.10.1016/j.tca.2008.03.018.

21. Beißmann S, Stiftinger M, Grabmayer K, Wallner G, Nitsche D, Buchberger W (2013) Monitoring the degradation of stabilization systems in polypropylene during accelerated aging tests by liquid chromatography combined with atmospheric pressure chemical ionization mass spectrometry. *Polym Degrad Stabil* 98: 1655-1661. https://doi.10.1016/j.polymdegradstab.2013.06.015.
22. Signoret C, Edo M, Lafon D, Caro-Bretelle AS, Lopez-Cuesta JM, Ienny P, Perrin D (2020) Degradation of styrenic plastics during recycling: Impact of reprocessing photodegraded material on aspect and mechanical properties. *J PolymEnviron* 28: 2055-2077. https://doi.10.1007/s10924-020-01741-8
23. Cardoso IN, Ranzan T, Kurek AP, Sellin N (2020) Recycling of chrome plated ABS parts pickled with nitric acid free solution. *J PolymEnviron* 28: 826-833. https:// doi:10.1007/s10924-019-01645-2 JOURNAL OF APPLIED POLYMER SCIENCE
24. Zhao Z, Wang Z, Zhang C, Wang Y, Li Z, Hu Y, Xiao X(2014) Polar polystyrene-isoprene-styrene copolymers with long polybutadiene branches. *J Appl Polym Sci* 131: 40303. https://doi.10.1002/app.40303.
25. Zhang J, Li L, Boonkerd K, Kim J K (2014) Formation of SBS triblock copolymers using waste soybean oil as coupling agent. *J Appl Polym Sci* 131: 40684. https://doi.10.1002/app.40684.
26. Zhang Z, Zhang L, Li Y, Xu H (2006) Styrene-butadiene-styrene/montmorillonite nanocomposites synthesized by anionic polymerization. *J Appl Polym Sci* 99: 2273-2278. https://doi.org/10.1002/app.22768.
27. Xicohtencatl-Serrano H, García-Leiner M, Cabrera-Ortiz A, Herrera-Nájera R (2014) Synthesis and characterization of poly (styrene-*b*-[(butadiene)$_{1-x}$-(ethylene-*co*-butylene)$_x$]-*b*-styrene) star-like molecular polymers produced by partial hydrogenation of SBS. *Polym Eng Sci* 54: 2332-2344. https://doi.10.1002/pen.23796.
28. Turner RR, Carlson DW,Altenau AG (1974) Determination of ungrafted rubber in ABS polymers. *J Elastom Plast* 6:94-102.
29. Shiundu PM, Remsen EE, Giddings JC (1996) Isolation and characterization of polymeric and particulate components of acrylonitrile-butadiene-styrene (ABS) plastics by thermal field-flow fractionation. *J Appl Polym Sci*60: 1695-1707. https://doi.10.1002/(SICI)1097-4628(19960606)60:10<1695::AID-APP22>3.0.CO;2-2.
30. Jaidev K, Biswal M, Mohanty S, Nayak SK (2021) Sustainable waste nanagement of engineering plastics generated from E-waste: A critical evaluation of mechanical, thermal and morphological properties. *J PolymEnviron*. https:doi.10.1007/s10924-020-01998-z

Figures

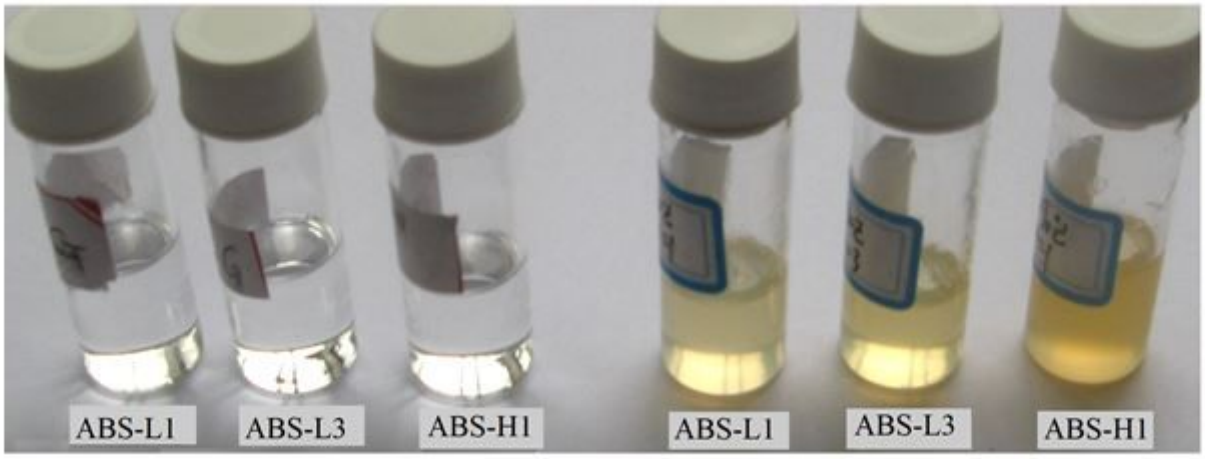

Figure 1

Photographs of suspensions and their filtrates

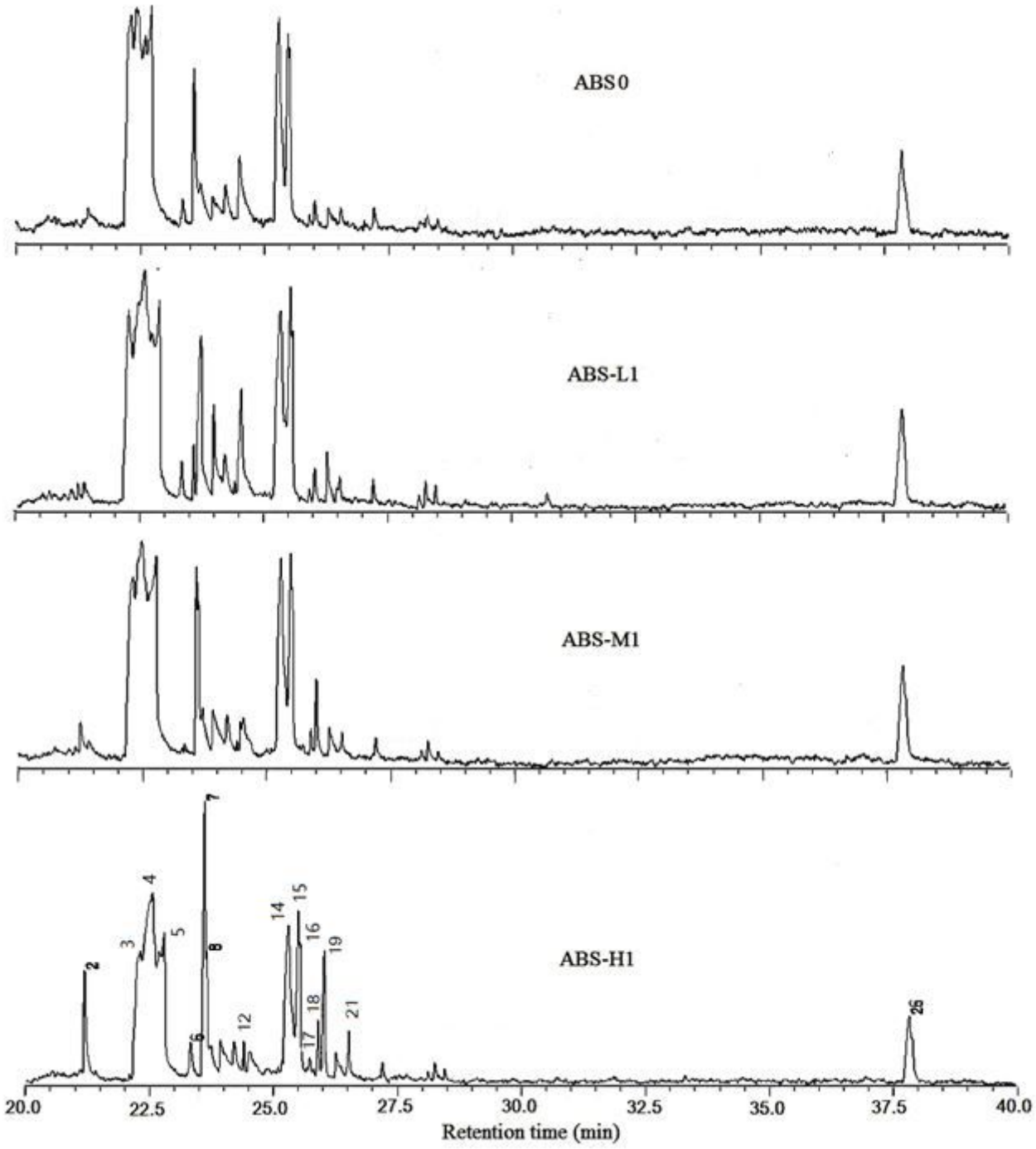

Figure 2

Total ion chromatograms of volatile compounds originating from virgin ABS, and ABS processed at 230, 260, and 290 °C

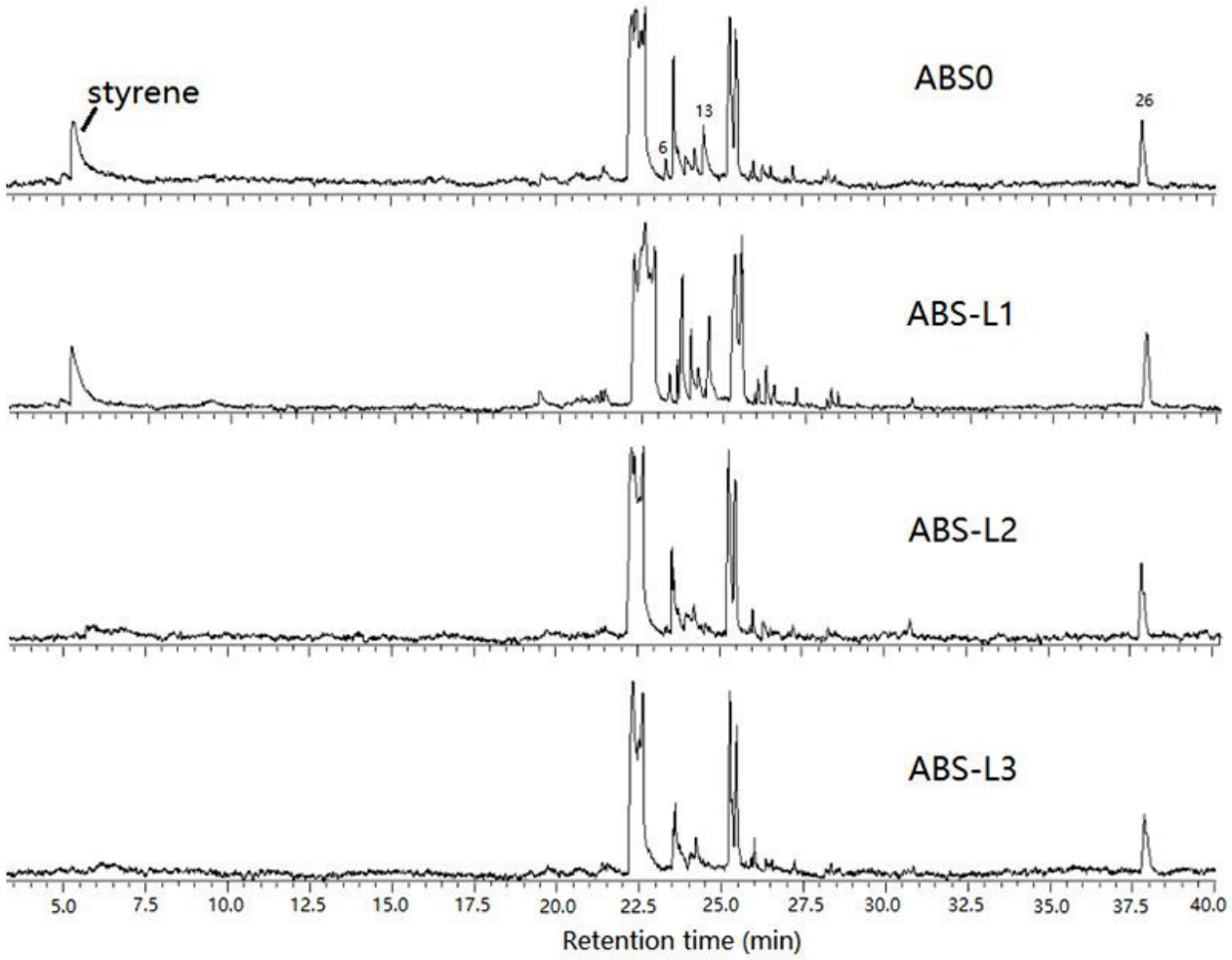

Figure 3

Total ion chromatograms of volatile compounds originating from virgin ABS, and ABS processed at 230 °C for different numbers of cycles

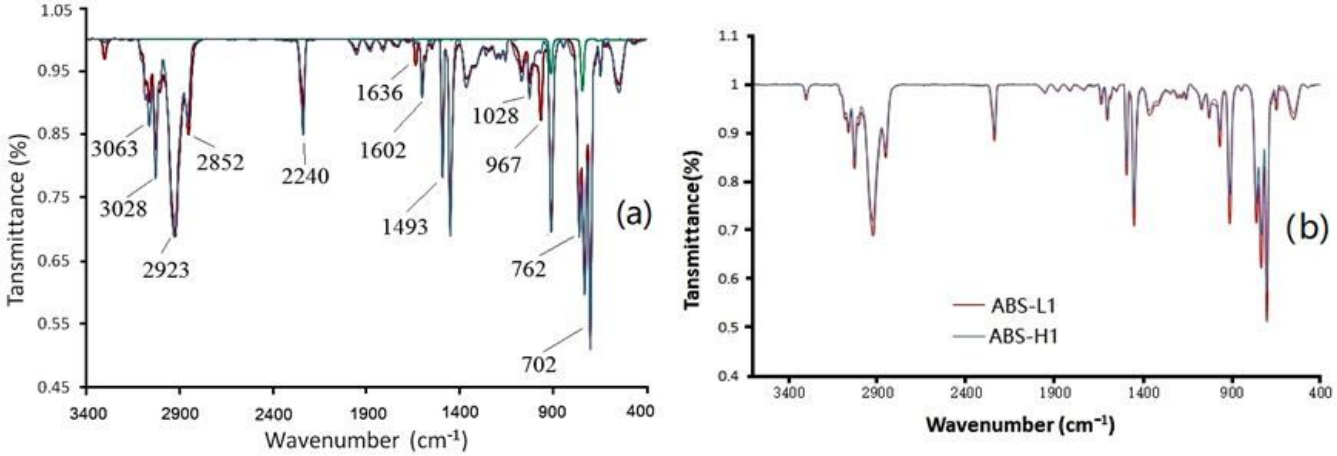

Figure 4

FTIR spectra of (a) ABS-L1 before (red) and after filtration (blue), and residual solvent (green), and (b) ABS suspensions after processing at 230 °C (red) and at 290 °C (blue) for one cycle

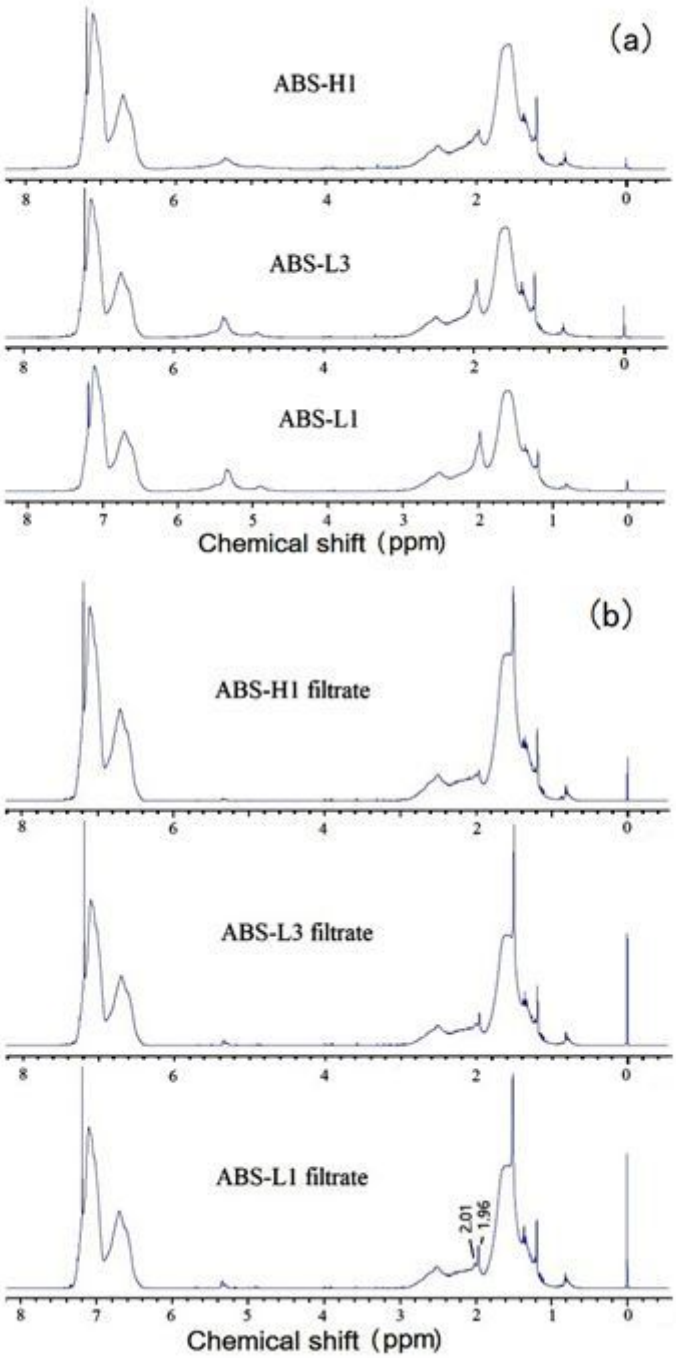

Figure 5

1H NMR spectra of (a) ABS suspensions, and (b) their filtrates after processing at different temperatures

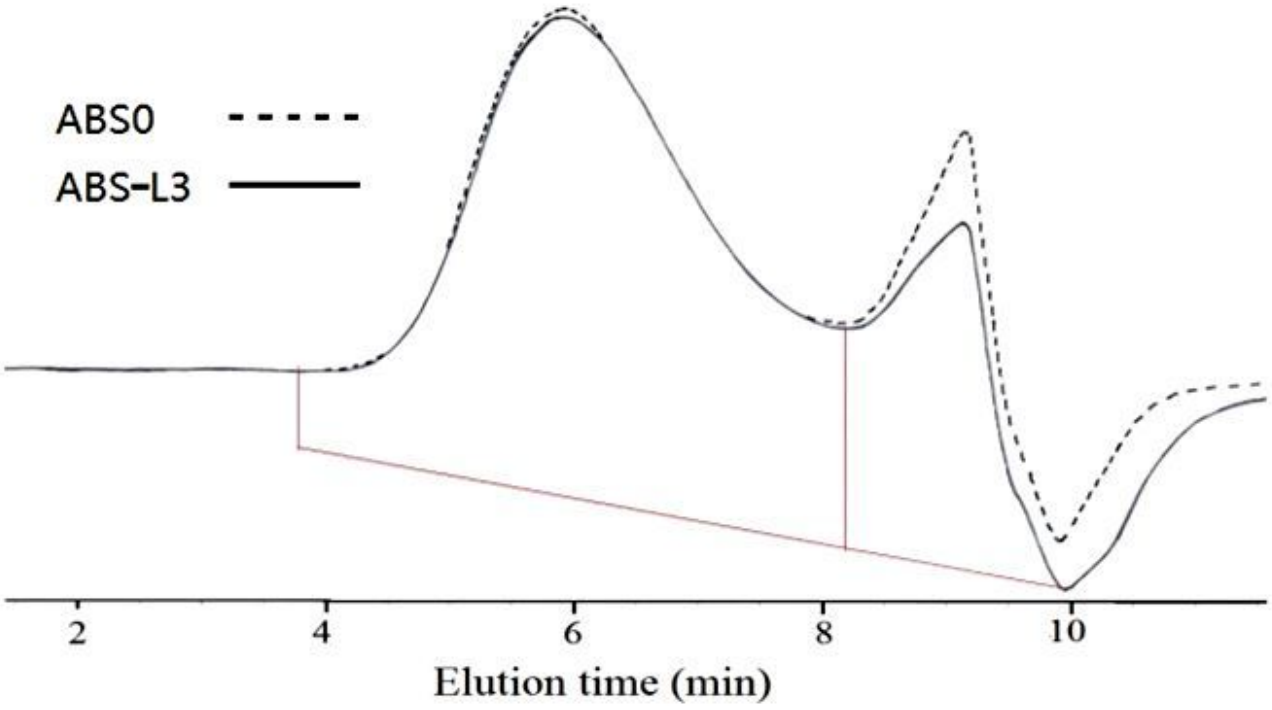

Figure 6

GPC curves of the soluble components of ABS before (dashed line) and after processing at 230 °C for three cycles (solid line)

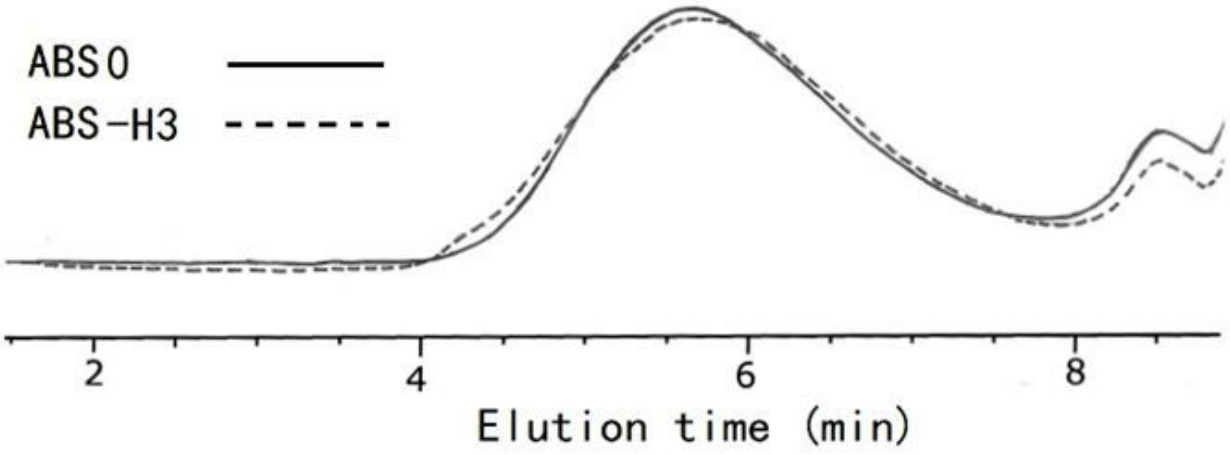

Figure 7

GPC curves of the soluble components of ABS before (solid line) and after processing at 290 °C for three cycles (dashed line)

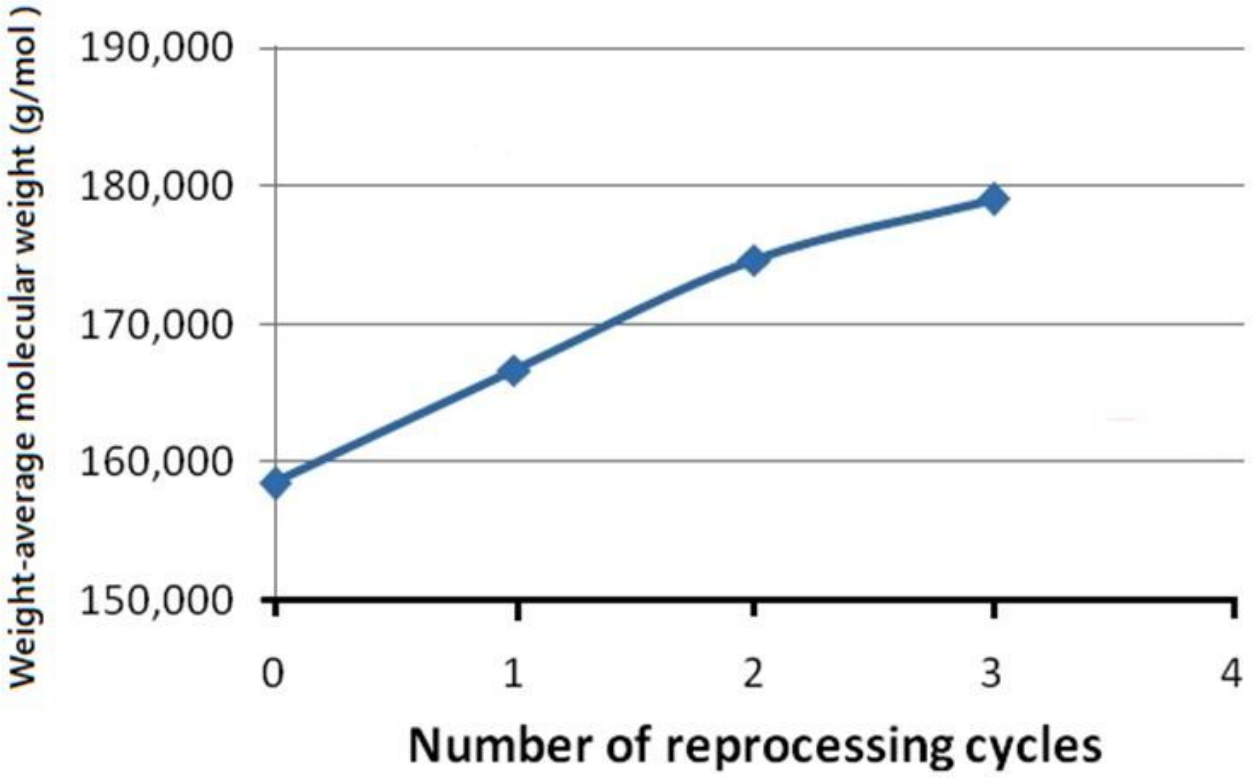

Figure 8

Mw of the soluble polymeric components of ABS after processing at 290 °C for different numbers of cycles

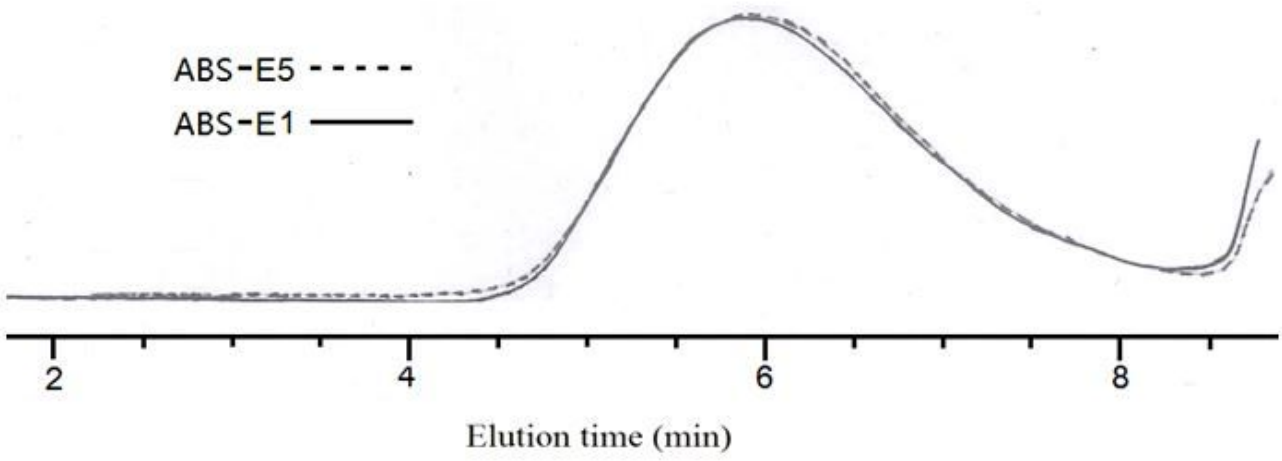

Figure 9

GPC curves of ABS-E1 (solid line) and ABS-E5 (dashed line)

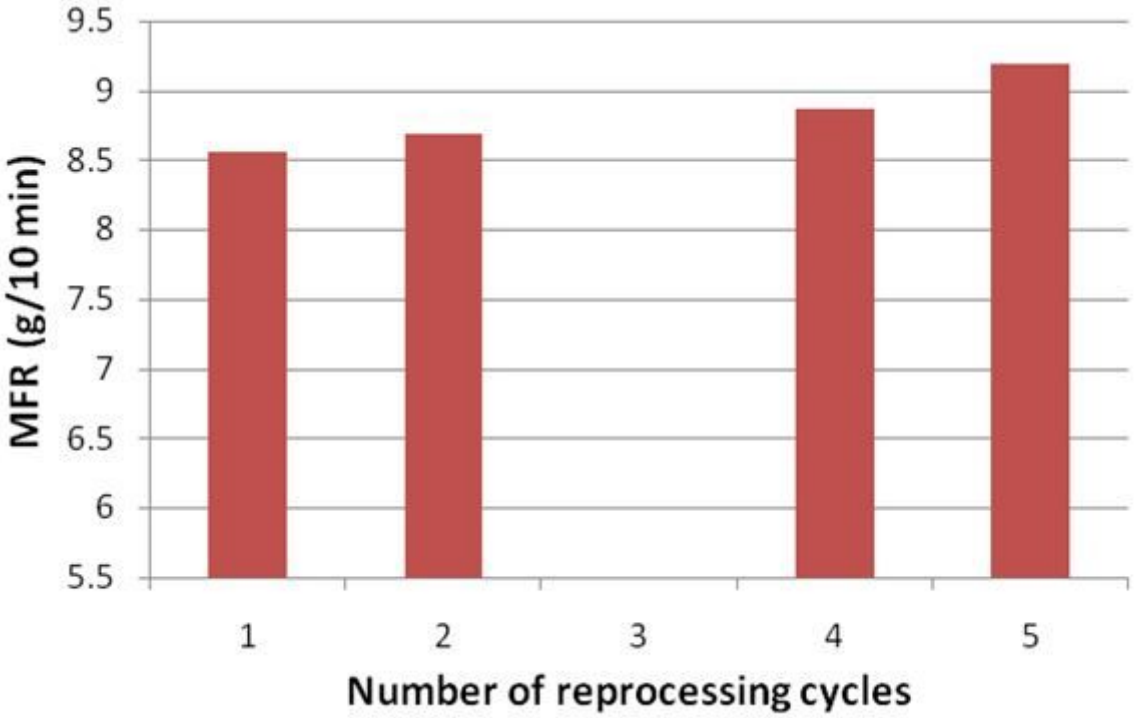

Figure 10

MFRs of ABS against number of processing cycles

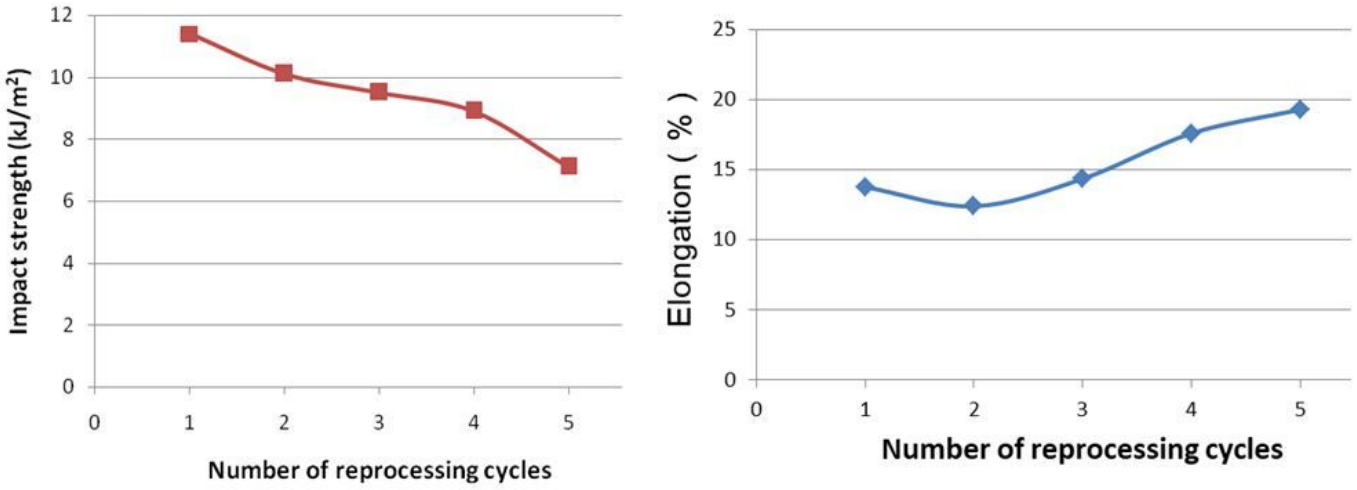

Figure 11

Impact strength and elongation of ABS against number of processing cycles

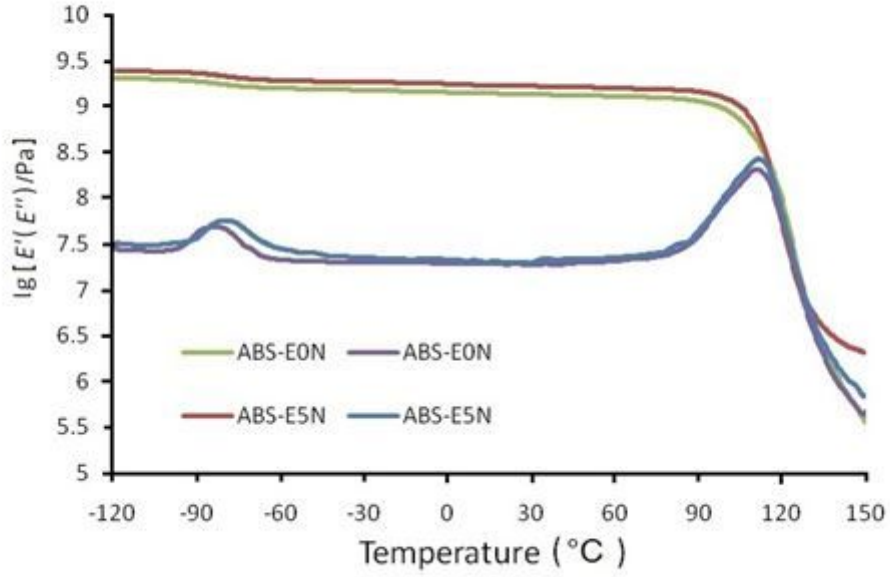

Figure 12

Lg E' (upper lines) and lg E" (lower lines) as functions of temperature for ABS-E0N and ABS-E5N

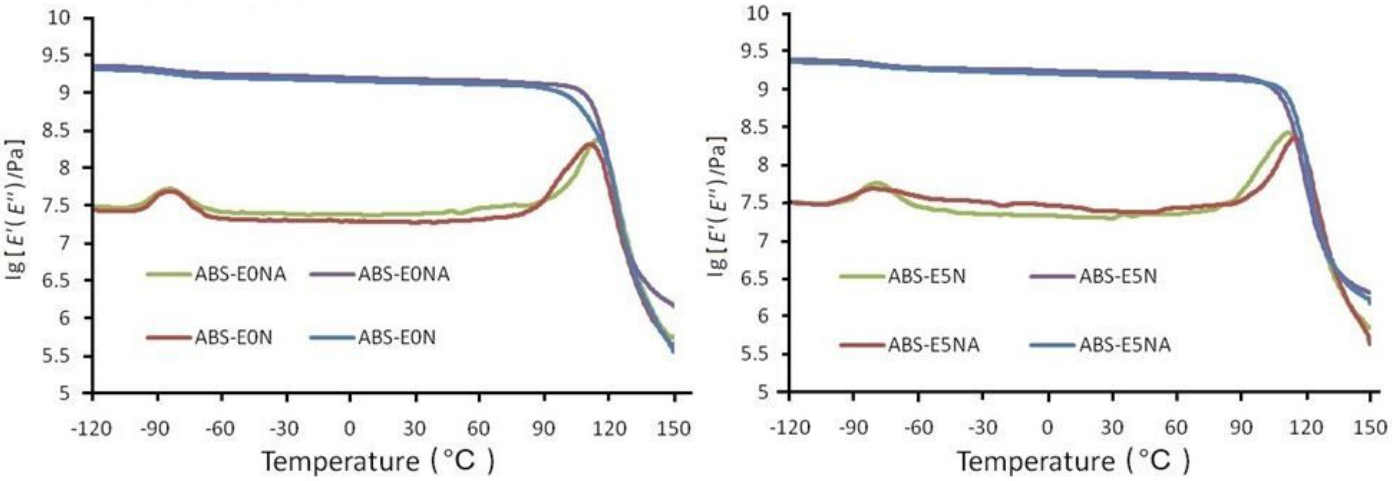

Figure 13

DMTA results for ABS-E0N and ABS-E0NA, and ABS-E5N and ABS-E5NA

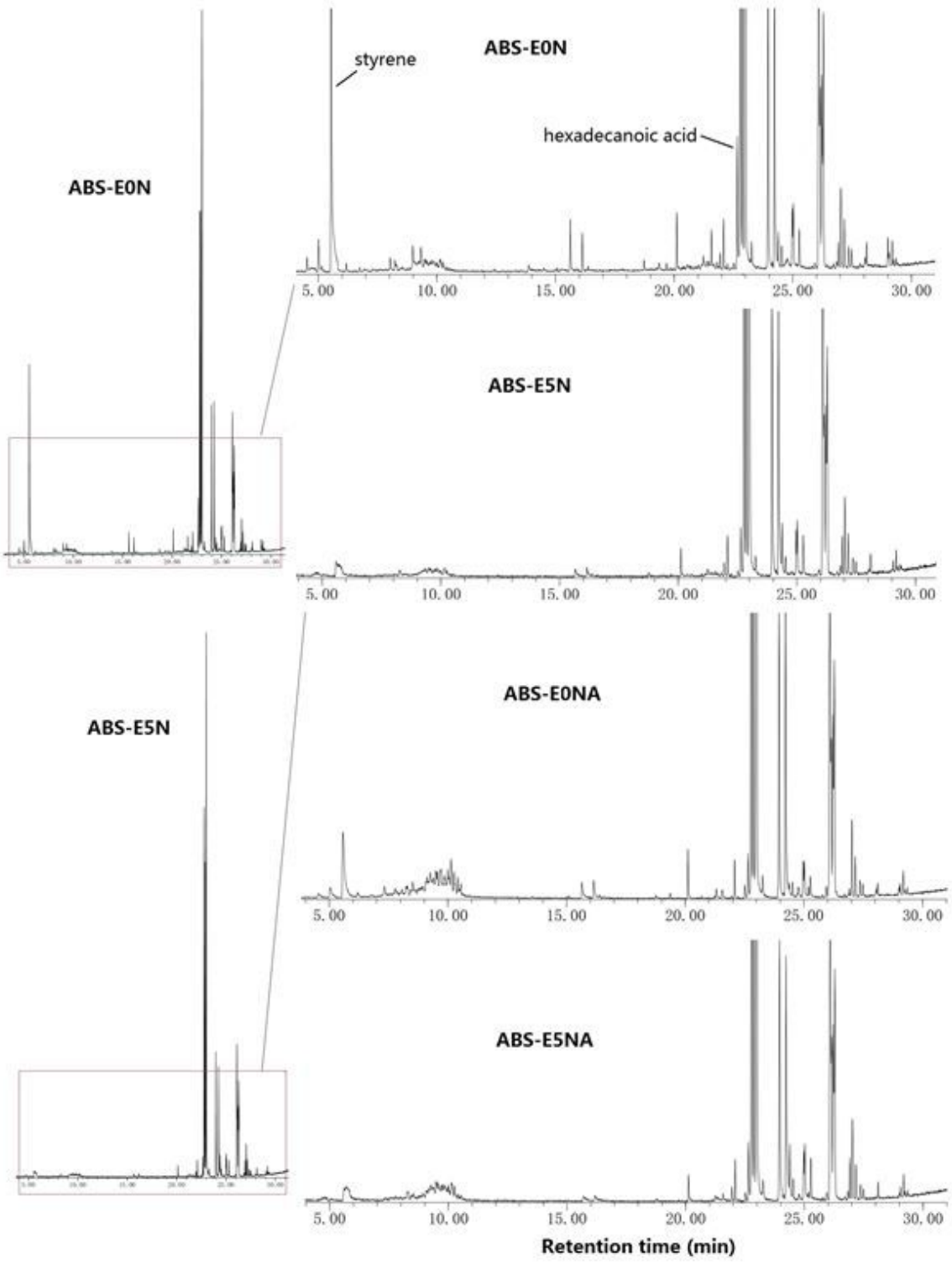

Figure 14

Total ion chromatograms of volatile compounds present in ABS-E0N, ABS-E5N, ABS-E0NA, and ABS-E5NA